Elastic properties of six silicate garnet end members from accurate ab initio simulations.

A. Erba, A. Mahmoud, R. Orlando, R. Dovesi
Elastic properties of six silicate garnet end members from accurate ab initio simulations.
PHYSICS AND CHEMISTRY OF MINERALS (2014) 41
DOI: 10.1007/s00269-013-0630-4

Noname manuscript No.
(will be inserted by the editor)

Elastic Properties of Six Silicate Garnet End-members from Accurate Ab initio Simulations.

Alessandro Erba · Agnes Mahmoud · Roberto Orlando · Roberto Dovesi

the date of receipt and acceptance should be inserted later

Abstract The elastic properties of six silicate garnet end-members, among the most important rock-forming minerals, are here investigated for the first time via accurate *ab initio* theoretical simulations. The CRYSTAL program is used which works within periodic boundary conditions and allows for all-electron basis sets to be adopted. From the computed elastic tensor, Christoffel's equation is solved along a set of crystallographic directions in order to fully characterize the seismic wave velocity anisotropy in such materials. Polycrystalline isotropic aggregate elastic properties are derived from the computed single-crystal data via the Voigt-Reuss-Hill averaging procedure. Transferability of the elastic properties from end-members to their solid solutions with different chemical compositions is also addressed.

Keywords Elastic constants · Garnet · Ab initio simulation · Elastic anisotropy

1 Introduction

Garnets constitute a large class of materials of great technological interest; they can be used as components of lasers, computer memories, microwave optical devices and, due to high hardness and recyclability, as abrasives and filtration media (Novak and Gibbs, 1971). Silicate garnets are among the most important rock-forming minerals and represent the main constituents of the Earth's lower crust, upper mantle and transition zone. They are characterized by a cubic structure with space group $Ia\overline{3}d$ and formula $X_3Y_2(SiO_4)_3$, where the X site hosts divalent cations such as Ca^{2+}, Mg^{2+}, Fe^{2+} and Mn^{2+} and the Y site is occupied by trivalent cations such as Al^{3+}, Fe^{3+} and Cr^{3+}. At least twelve end-members of this family of minerals have been identified (Rickwood et al, 1968). The primitive cell contains four formula units (80 atoms) and the structure consists in alternating SiO_4 tetrahedra and YO_6 octahedra sharing corners to form a three-dimensional network. The most common end-members of the family are pyrope $Mg_3Al_2(SiO_4)_3$, almandine $Fe_3Al_2(SiO_4)_3$, spessartine $Mn_3Al_2(SiO_4)_3$, grossular $Ca_3Al_2(SiO_4)_3$, uvarovite $Ca_3Cr_2(SiO_4)_3$ and andradite $Ca_3Fe_2(SiO_4)_3$. Natural silicate garnets can be found in a wide range of chemical compositions since they form solid solutions. In particular, the aluminosilicate garnets with different X cations show complete solid solubility among them at high pressure (O'Neill et al, 1989).

Different geological models have been proposed for the Earth's upper mantle: in the pyrolite model (Ringwood, 1975) the entire upper mantle is chemically homogeneous and the garnet phase would be mainly composed by a pyralspite (pyrope-almandine-spessartine) solid solution; in the piclogite models (Bass and Anderson, 1984; Anderson and Bass, 1986) the transition region between 400 and 670 km depth would be richer in calcium and with more abundant garnets than the pyrolite model. Modern seismology has become an instrument for accurate experimental measurements of the elastic properties of the Earth's deep interior that can help in discriminating among different compositional models, provided the elastic properties of the individual constituents are well-characterized. It is clear that an accurate and complete determination of the elastic properties of the six silicate garnet end-members listed above and their possible solid solutions at ambi-

A. Erba · A. Mahmoud · R. Orlando · R. Dovesi
Dipartimento di Chimica and Centre of Excellence NIS (Nanostructured Interfaces and Surfaces), Università di Torino, via Giuria 5, IT-10125 Torino (Italy)
Tel.: +39 011 6707562
E-mail: alessandro.erba@unito.it

ent and geophysical (high pressure, high temperature) conditions, would represent a significant progress in this kind of studies.

With this paper we begin a systematic, theoretical study, at the *ab initio* quantum-chemical level, of the elastic properties of silicate garnets. Through this kind of simulations, not only mean aggregate properties (bulk modulus, elastic constants, etc.), but also directional single-crystal seismic velocities and anisotropies can be computed accurately. Before predicting their elastic properties at high pressure, we perform theoretical simulations at ambient conditions in order to define a reliable computational setup. The elastic properties of silicate garnets at ambient conditions have been measured experimentally for pyrope (Isaak and Graham, 1976; Bonczar et al, 1977; Leitner et al, 1980; O'Neill et al, 1989, 1991; Sinogeikin and Bass, 2000; Duffy and Anderson, 1989; Chen et al, 1999; Chopelas et al, 1996; Wang and Ji, 2001; Lu et al, 2013), almandine (Isaak and Graham, 1976; O'Neill et al, 1989; Wang and Ji, 2001), spessartine (Isaak and Graham, 1976; Bass, 1989; Sumino and Anderson, 1982), grossular (Isaak and Graham, 1976; Bass, 1989; Wang and Ji, 2001; Halleck, 1973), uvarovite (Bass, 1986; Wang and Ji, 2001) and andradite (Bass, 1986; Wang and Ji, 2001; Jiang et al, 2004). Most of these studies refer to polycrystalline aggregates while few of them report accurate single-crystals directional seismic velocities and anisotropies (Jiang et al, 2004; Bass, 1989; O'Neill et al, 1991).

Previous studies analyzed the transferability of elastic properties (bulk modulus, shear modulus, Poisson ratio, etc.) from silicate garnet end-members to their solid solutions displaying different chemical compositions (Isaak and Graham, 1976; Duffy and Anderson, 1989; Yeganeh-Haeri et al, 1990). In particular, linear composition-bulk modulus trends are observed for garnets in the pyralspite system; large deviations from the linear regime have been reported for solid solutions between grossular and andradite (Babuška et al, 1978; O'Neill et al, 1989). Solid solutions between pyralspites and ugrandites (uvarovite-grossular-andradite) are quite rare in natural garnets (Hensen, 1976). The transferability of our *ab initio* computed elastic properties of the six end-members towards possible solid solutions is here discussed and quantified. An explicit quantum-chemical description of pressure and solid solubility effects on silicate garnets is currently under way.

Only a few theoretical investigations of elastic properties of garnets can be found in the literature. Winkler et al (1991) performed lattice dynamical calculations with semiempirical potentials and computed ambient pressure elastic constants of pyrope and grossular that were overestimated by about 20 %. Quasi-harmonic lattice dynamical simulations, based on an empirical potential, were performed by Pavese (1999) to compute elastic constants of pyrope at ambient conditions and pressure dependent bulk modulus. Mittal et al (2001) used a shell-model semiempirical interatomic potential and reported lattice dynamical calculations of elastic constants of four end-members (pyrope, grossular, spessartine and almandine). Two *ab initio* studies are reported: Li and Weidner (2011) performed molecular dynamics simulations of the elastic constants of pyrope, as a function of pressure and temperature, in a projector-augmented-waves (PAW) density-functional-theory (DFT) implementation; Kawai and Tsuchiya (2012) performed DFT calculations of the elastic properties of grossular, in the local-density approximation (LDA).

In this paper, we report the full set of the elastic properties of six silicate garnet end-members, computed *ab initio* using a fully periodic implementation of the hybrid B3LYP, Becke-three parameters-Lee-Yang-Parr, (Becke, 1993; Lee et al, 1988) functional and all-electron basis sets. The same computational approach was successfully applied to the investigation of structural, electronic, vibrational (Infrared and Raman), magnetic and optical properties of silicate garnets (D'Arco et al, 1996; Dovesi et al, 2011; Zicovich-Wilson et al, 2008; Meyer et al, 2010; Valenzano et al, 2009, 2010; Lacivita et al, 2013a). Calculations are performed with a development version of the CRYSTAL program (Dovesi et al, 2010, 2005) where a fully-automated and general procedure for computing elastic tensors, photoelastic constants and seismic velocities of crystals of any symmetry has recently been implemented and applied to the study of several crystals (Perger et al, 2009; Erba et al, 2013b; Lacivita et al, 2013b; Erba et al, 2013a; Baima et al, 2013; Erba and Dovesi, 2013).

The structure of the paper is as follows: In Section 2, the computational scheme adopted, as well as the relations among the main elastic properties to be discussed, are presented. The computed elastic properties, at ambient pressure, of the six silicate garnet end-members here considered are presented in Section 3; in particular, their elastic anisotropy is discussed in Section 3.1. Section 3.2 is devoted to the investigation of the possible transferability of elastic properties from pure end-members to solid solutions of different chemical composition. Final remarks are given in Section 4.

2 Computational Techniques and Details

2.1 Elastic Constants and Related Properties

The elements of the fourth-rank elastic tensor C for 3D systems are usually defined as second energy density derivatives with respect to pairs of deformations (Nye, 1957):

$$C_{vu} = \frac{1}{V}\left.\frac{\partial^2 E}{\partial\eta_v \partial\eta_u}\right|_0 , \qquad (1)$$

where $\boldsymbol{\eta}$ is the symmetric second-rank pure strain tensor and Voigt's notation is used according to which $v, u = 1, \ldots 6$ ($1 = xx$, $2 = yy$, $3 = zz$, $4 = yz$, $5 = xz$, $6 = xy$). An automated scheme for the calculation of C (and of $\mathsf{S} = \mathsf{C}^{-1}$, the compliance tensor) has been implementation in the CRYSTAL program (Perger et al, 2009). The elastic C tensor exhibits, in general, 21 independent elements that reduce to 3 (*i.e.* C_{11}, C_{12} and C_{44}) for crystals with cubic symmetry, as in the case of silicate garnets. We recall that elastic constants can be decomposed into purely electronic "clamped-ion" and nuclear "internal-strain" contributions; the latter measures the effect due to relaxation of the relative positions of atoms induced by the strain (Saghi-Szabo et al, 1998; Dal Corso et al, 1994) and can be computed simply by optimizing the atomic positions within the strained cell.

Some elastic properties of an isotropic polycrystalline aggregate can be computed from the elastic and compliance constants defined above via the Voigt-Reuss-Hill averaging scheme (Hill, 1963). For cubic crystals, the adiabatic bulk modulus K_S is simply defined as:

$$K_S = {}^1\!/_3(C_{11} + 2C_{12}) \equiv {}^1\!/_3(S_{11} + 2S_{12})^{-1} . \qquad (2)$$

The shear modulus $\overline{G} = {}^1\!/_2[G_V + G_R]$ can be expressed as the average between Voigt upper G_V and Reuss lower G_R bounds as:

$$\overline{G} = {}^1\!/_{10}(C_{11} - C_{12} + 3C_{44}) + {}^5\!/_2(4(S_{11} - S_{12}) + 3S_{44})^{-1} .$$

From the bulk modulus and the average shear modulus defined above, Young's modulus E and Poisson's ratio σ can be defined as well:

$$E = \frac{9K_S\overline{G}}{3K_S + \overline{G}} \quad \text{and} \quad \sigma = \frac{3K_S - 2\overline{G}}{2(3K_S + \overline{G})} . \qquad (3)$$

According to the elastic continuum theory, the three acoustic wave velocities of a crystal, along any general direction represented by unit wave-vector $\hat{\mathbf{q}}$, are related to the elastic constants by Christoffel's equation which can be given an eigenvalues/eigenvectors form as follows (Musgrave, 1970; Auld, 1973):

$$\mathbf{A}^{\hat{\mathbf{q}}}\mathbf{U} = \mathbf{V}^2\mathbf{U} \qquad \text{with} \qquad A^{\hat{\mathbf{q}}}_{kl} = \frac{1}{\rho}\hat{q}_i C_{iklj}\hat{q}_j , \qquad (4)$$

where ρ is the crystal density, $i, j, k, l = x, y, z$ represent Cartesian directions, $\hat{q}_i$ is the i-th element of the unit vector $\hat{\mathbf{q}}$, $\mathbf{V}$ is a 3×3 diagonal matrix whose three elements give the acoustic velocities and $\mathbf{U} = (\hat{\mathbf{u}}_1, \hat{\mathbf{u}}_2, \hat{\mathbf{u}}_3)$ is the eigenvectors 3×3 matrix where each column represents the polarization $\hat{\mathbf{u}}$ of the corresponding eigenvalue. The three acoustic wave velocities, also referred to as seismic velocities, can be labeled as quasi-longitudinal v_p, slow quasi-transverse v_{s1} and fast quasi-transverse v_{s2}, depending on the polarization direction $\hat{\mathbf{u}}$ with respect to wave-vector $\hat{\mathbf{q}}$ (Karki et al, 2001).

Again, within the Voigt-Reuss-Hill averaging scheme, the average values of transverse (shear) and longitudinal seismic wave velocities, for an isotropic polycrystalline aggregate, can be computed from the elastic constants and the density ρ of the crystal as (Ottonello et al, 2010):

$$\overline{v}_s = \sqrt{\frac{\overline{G}}{\rho}} \quad \text{and} \quad \overline{v}_p = \sqrt{\frac{K_S + {}^4\!/_3\overline{G}}{\rho}} . \qquad (5)$$

A further elastic property of great interest is the so-called elastic wave anisotropy which can be measured by the dimensionless parameter A that vanishes for an isotropic material, according to the following relation:

$$\frac{v^2_{[111]}}{v^2_{[100]}} - 1 = \alpha A , \qquad (6)$$

where $v_{[hkl]}$ is the velocity with which a seismic wave propagates along the $[hkl]$ crystallographic direction (*i.e.* $\mathbf{q} = h\mathbf{a}_1 + k\mathbf{a}_2 + l\mathbf{a}_3$, with h, k, l Miller's indices and $\mathbf{a}_i$, for $i = 1, 2, 3$ direct lattice vectors) and α a coefficient for the specific wave type: p, $s1$ or $s2$ (Karki et al, 1997; Tsuchiya and Kawamura, 2001). For cubic crystals, seismic wave velocities along high symmetry directions, such as $v_{[111]}$ and $v_{[100]}$, can be computed with simple analytical expressions in terms of the elastic constants (Authier and Zarembowitch, 2006); as a consequence, the elastic wave anisotropy A can be given the following simple form:

$$A = \frac{2C_{44} + C_{12}}{C_{11}} - 1 . \qquad (7)$$

Even cubic crystals show a non-zero elastic wave anisotropy. A recent *ab initio* investigation of the elastic anisotropy of α-Al_2O_3 has been performed by Belmonte et al (2013).

2.2 Computational Parameters

All the calculations reported in this manuscript are performed with a development version of the program CRYSTAL for *ab initio* quantum chemistry of solid state (Dovesi et al, 2010, 2005). All-electron atom-centered Gaussian-type-function (GTF) basis sets are adopted. Oxygen atoms are described by a (8s)-(411sp)-(1d) contraction of primitive GTFs, silicon by a (8s)-(6311sp)-(1d) one, aluminum by a (8s)-(611sp)-(1d) one, calcium by a (8s)-(6511sp)-(21d) one and magnesium by a (8s)-(511sp)-(1d) one. For transition metal ions (manganese, iron and chrome), a (8s)-(64111sp)-(411d) contraction of GTFs is used, augmented with a further f-type polarization function as reported into details in previous works (Zicovich-Wilson et al, 2008; Pascale et al, 2005; Dovesi et al, 2011). The popular B3LYP one-electron Hamiltonian is adopted, which contains a hybrid Hartree-Fock/Density-Functional exchange-correlation term. It has been widely and successfully used in computational quantum chemistry (Koch and Holthausen, 2000) since it describes many structural, electronic and vibrational features of molecules and crystals in good agreement with experimental data (Zicovich-Wilson et al, 2008; Tosoni et al, 2005).

In CRYSTAL, the truncation of infinite lattice sums is controlled by five thresholds, which are set to 7 7 7 7 16 (Dovesi et al, 2010). Reciprocal space is sampled according to a sub-lattice with shrinking factor 3, corresponding to 4 points in the irreducible Brillouin zone. The DFT exchange-correlation contribution is evaluated by numerical integration over the cell volume: radial and angular points of the atomic grid are generated through Gauss-Legendre and Lebedev quadrature schemes, using an accurate predefined pruned grid: the accuracy in the integration procedure can be estimated by evaluating the error associated with the integrated electronic charge density in the unit cell versus the total number of electrons per cell: 2 $\times 10^{-5}|e|$ out of a total number of 800 electrons per cell for pyrope, for instance. The convergence threshold on energy for the self-consistent-field (SCF) step of the calculations is set to 10^{-10} hartree. In the case of almandine, in order to get rid of an extremely slow convergence of the SCF procedure, due to the Jahn-Teller nature of its ground state, which is related to the d^6 electronic configuration of the Fe^{2+} cation, a Broyden convergence accelerator scheme has been adopted.

Equilibrium and strained configurations are optimized by use of analytical energy gradients calculated with respect to both atomic coordinates and unit-cell parameters or atomic coordinates only, respectively (Doll, 2001; Doll et al, 2001; Civalleri et al, 2001). A quasi-Newtonian technique is used, combined with the BFGS algorithm for Hessian updating (Broyden, 1970; Fletcher, 1970; Goldfarb, 1970; Shanno, 1970). Convergence is checked on both gradient components and nuclear displacements; the corresponding tolerances on their root mean square are chosen to be 10 times more severe than the default values for simple optimizations: 0.00003 a.u. and 0.00012 a.u., respectively. For the elastic constants calculation, two strained configurations are considered for each independent strain, with a dimensionless strain amplitude of 0.01.

3 Results and Discussion

In this section we report and discuss the results of accurate *ab initio* simulations, as performed with the B3LYP hybrid functional, of the elastic properties of silicate garnets, at ambient pressure. The computed elastic constants and bulk moduli are first compared with the outcomes of previous experimental and theoretical (when available) determinations, which are here reviewed. A detailed theoretical description of the elastic wave anisotropy of the end-members is then presented. From our single-crystal computed values, average elastic properties are computed for isotropic polycrystalline aggregates, via the Voigt-Reuss-Hill procedure. Finally, the transferability of the elastic properties from pure end-members to a large set of solid solutions is discussed and compared with available experimental data.

In Table 1, we report our computed values of the elastic constants and bulk modulus of six silicate garnet end-members, pyrope, (Pyr), almandine (Alm), spessartine (Spe), grossular (Gro), andradite (And) and uvarovite (Uva) at ambient pressure, along with previous experimental and theoretical results for comparison; the corresponding references are given in the table as well. Experimental results are reported for each end-member in the upper box.

Pyrope $Mg_3Al_2(SiO_4)_3$ is by far the most studied garnet: seven experimental (Isaak and Graham, 1976; Bonczar et al, 1977; Leitner et al, 1980; O'Neill et al, 1989, 1991; Sinogeikin and Bass, 2000; Lu et al, 2013) and three theoretical (Pavese, 1999; Winkler et al, 1991; Mittal et al, 2001) studies are reviewed. Experimental data show a certain spread, but the most recent three studies are quite homogeneous (O'Neill et al, 1989, 1991; Sinogeikin and Bass, 2000). The agreement between the last three and our computed values is remarkable. Previous theoretical data, computed with semiempirical potentials, perform poorly and overshoot the elastic constants. Two experimental works are available for almandine $Fe_3Al_2(SiO_4)_3$ (Isaak and Graham, 1976; O'Neill et al, 1989); the latter one is the most accurate

Table 1 Elastic constants C_{vu} (GPa) and adiabatic bulk modulus K_S (GPa) of the six silicate garnet end-members here considered. Present computed values are compared with previously measured experimental (above the horizontal line) and simulated (below lines) data. Few details about the techniques used in each cited work are given (RTP stands for room temperature and pressure).

	Ref.	Technique	C_{11}	C_{12}	C_{44}	K_S
Pyr	Isaak *et al.* (1976)	Ultrasonic, at RTP	287	105	92	166
	Bonczar *et al.* (1977)	Ultrasonic, at RTP	292	106	92	168
	Leitner *et al.* (1980)	Brillouin scattering, at RTP	295	117	90	177
	O'Neill *et al.* (1989)	Brillouin scattering, at RTP	296	111	92	173
	O'Neill *et al.* (1991)	Brillouin scattering, at RTP	298	110	93	172
	Sinogeikin *et al.* (2000)	Brillouin scattering, at RTP	297	108	93	171
	Lu *et al.* (2013)	Brillouin scattering, at RTP	291	107	92	168
	Pavese (1999)	Empirical potentials	298	113	93	174
	Winkler *et al.* (1999)	Semiempirical potentials	339	132	115	201
	Mittal *et al.*(2001)	Semiempirical potentials	314	116	91	182
	This study	Ab initio B3LYP	**296**	**109**	**89**	**171**
Alm	Isaak *et al.* (1976)	Ultrasonic, at RTP	310	115	93	180
	O'Neill *et al.* (1989)	Brillouin scattering, at RTP	309	111	96	177
	Mittal *et al.* (2001)	Semiempirical potentials	318	113	90	182
	This study	Ab initio B3LYP	**306**	**108**	**88**	**174**
Spe	Isaak *et al.* (1976)	Ultrasonic, at RTP	302	108	96	172
	Bass (1989)†	Brillouin scattering, at RTP	310	114	95	179
	Mittal *et al.* (2001)	Semiempirical potentials	313	109	89	177
	This study	Ab initio B3LYP	**310**	**114**	**94**	**179**
Gro	Halleck (1973)	Ultrasonic, at RTP	318	98	101	171
	Isaak *et al.* (1976)	Ultrasonic, at RTP	320	96	102	171
	Bass (1989)‡	Brillouin scattering, at RTP	322	91	105	168
	Winkler *et al.* (1999)	Semiempirical potentials	397	98	94	198
	Mittal *et al.* (2001)	Semiempirical potentials	305	103	84	170
	Kawai *et al.* (2012)	Ab initio LDA	334	98	104	177
	This study	Ab initio B3LYP	**323**	**95**	**105**	**171**
And	Bass (1986)	Brillouin scattering, at RTP	289	92	85	157
	Jiang *et al.* (2004)	Brillouin scattering, at RTP	284	88	83	155
	This study	Ab initio B3LYP	**281**	**88**	**83**	**152**
Uva	Bass (1986)	Brillouin scattering, at RTP	304	91	84	162
	This study	Ab initio B3LYP	**306**	**83**	**87**	**157**

† Extrapolated from a 95 % Spessartine sample
‡ Extrapolated from a 99 % Grossular sample

and the agreement with our computed data is again good, apart from a slight underestimation of the theoretical values, particularly so for the C_{44} constant. Two experimental sets of values are reported for spessartine $Mn_3Al_2(SiO_4)_3$; the latter by Bass (1989), even if extrapolated from a 95 % only spessartine sample, is the most reliable. In this case the agreement with our computed elastic properties is excellent. The computed values for grossular $Ca_3Al_2(SiO_4)_3$ are in close agreement with the three experimental datasets reported in the table (Isaak and Graham, 1976; Bass, 1989; Halleck, 1973). Previous theoretical simulations, based on semiempirical potentials, (Winkler et al, 1991; Mittal et al, 2001) predicted definitely wrong elastic properties of grossular, while a previous LDA study (Kawai and Tsuchiya, 2012) gave a reasonable description, as can be seen from the table. Two experiments are reported in the table for andradite $Ca_3Fe_2(SiO_4)_3$ (Bass, 1986; Jiang et al, 2004); the second one is particularly accurate and provides reliable seismic wave directional data (*vide infra*). The agreement between our theoretical predictions and these data is again remarkable. Only one experimental study is available for uvarovite $Ca_3Cr_2(SiO_4)_3$ at ambient pressure (Bass, 1986); in this case the agreement is still good but slightly worse than for the previous end-members.

From the computed elastic constants reported in Table 1, we determined a number of average elastic properties for isotropic polycrystalline aggregates of the six silicate garnet end-members: average shear modulus $\overline{G}$, Young's modulus E, Poisson's ratio σ, transverse $\overline{v}_s$ and longitudinal $\overline{v}_p$ seismic wave velocities are reported in Table 2 (see Section 2.1 for definitions).

For each garnet we also computed the "clamped-ion", purely electronic, contribution to all the quantities considered, as obtained by keeping atomic positions fixed within the strained cell during the elastic tensor calculation. We find that the purely electronic term is providing very high values of bulk moduli (219 GPa for pyrope, 224 GPa for Almandine, 193 GPa for Uvarovite,

Table 2 Elastic properties of the six silicate garnet end-members here considered, as computed *ab initio* in the present study: density ρ, average polycrystalline shear modulus $\overline{G}$, Young's modulus E, Poisson's ratio σ, average polycrystalline transverse $\overline{v}_s$ and longitudinal $\overline{v}_p$ seismic wave velocities and seismic wave anisotropy A.

	ρ (g/cm^3)	$\overline{G}$ (GPa)	E (GPa)	σ	$\overline{v}_s$ (km/s)	$\overline{v}_p$ (km/s)	A
Pyr	3.47	91	231	0.27	5.118	9.180	-0.031
Alm	4.19	93	236	0.27	4.703	8.429	-0.070
Spe	4.09	96	244	0.27	4.839	8.664	-0.025
Gro	3.51	109	269	0.24	5.573	9.496	-0.055
And	3.73	88	222	0.26	4.866	8.504	-0.098
Uva	3.72	96	240	0.25	5.087	8.762	-0.159

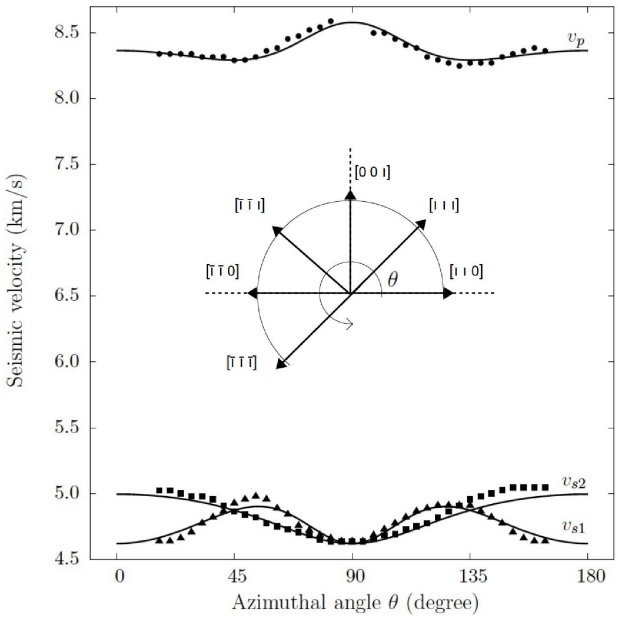

Fig. 1 Directional seismic wave velocities of an andradite $Ca_3Fe_2(SiO_4)_3$ single-crystal, as computed *ab initio* in the present study (continuous lines) and as measured by Brillouin scattering at ambient pressure by Jiang et al (2004) (black symbols). Seismic wave velocities (quasi-longitudinal v_p, slow and fast quasi-transverse v_{s1} and v_{s2}) are reported along an azimuthal angle θ defined in the inset. Computed values are downshifted by 0.1 km/s.

for instance), which are then significantly corrected by the nuclear relaxation term, down to 171 GPa, 174 GPa and 157 GPa, respectively. The nuclear relaxation contribution is then found to be very important for this class of materials. For simple symmetry reasons, other materials, such as MgO, NaCl and cubic $SrTiO_3$, for instance, are characterized by a null nuclear relaxation term (Erba and Dovesi, 2013; Erba et al, 2013a).

3.1 Elastic Anisotropy

Table 2 provides information about the elastic anisotropy of silicate garnet end-members. In the last column, we report the computed seismic wave anisotropy A, as defined by the relations (6 - 7). This quantity would be zero for an ideal isotropic substance. The elastic anisotropy of garnets is rather small (0.6 % and 1 % for p and s seismic wave velocities, respectively), if compared to that of other rock-forming minerals as olivine (25 % and 22 %), spinel (12 % and 68 %), muscovite (58 % and 85 %), orthopyroxene (16 % and 16 %), etc (Anderson, 1989). From the analysis of these values we can sort the six silicate garnet end-members according to their increasing elastic anisotropy: Spe < Pyr < Gro < Alm < And $\ll$ Uva. Spessartine and pyrope show very low anisotropy (A = -0.025 and A = -0.031, respectively) while uvarovite is by far the most anisotropic among them (A = -0.159). Once the elastic tensor has been computed, directional seismic wave velocities can be obtained by solving Christoffel's equation (4). In Figure 1, we compare our *ab initio* determinations of directional seismic wave velocities of andradite $Ca_3Fe_2(SiO_4)_3$ with the outcomes of an accurate single-crystal Brillouin scattering experiment, at ambient pressure, reported by Jiang et al (2004). Seismic wave velocities (quasi-longitudinal v_p, slow and fast quasi-transverse v_{s1} and v_{s2}) are reported along an azimuthal angle θ defined in the inset of the figure: $\theta = 0°$ corresponds to the crystallographic direction [110], $\theta = 45°$ to the [111] direction, $\theta = 90°$ to the [001] direction, etc. From inspection of the figure, it is clearly seen how accurately the description of both the angular dependence and the oscillation amplitudes of the seismic wave velocities are reproduced.

In Figure 2, we report our ab initio computed directional seismic wave velocities for the six silicate garnet end-members along the same azimuthal angle θ defined in the inset of Figure 1. The information about the elastic anisotropy embodied by index A, reported in Table 1, is found also in the data reported in the figure. Spessartine and pyrope show a rather isotropic behavior with seismic wave velocities which are almost independent of the crystallographic directions, represented by angle θ; uvarovite (dashed curves) clearly shows the largest anisotropy. From the analysis of the quasi-longitudinal, primary, velocities v_p in the figure, we can sort the six end-members according to increasing propagation velocity as: Alm < And < Spe < Uva <

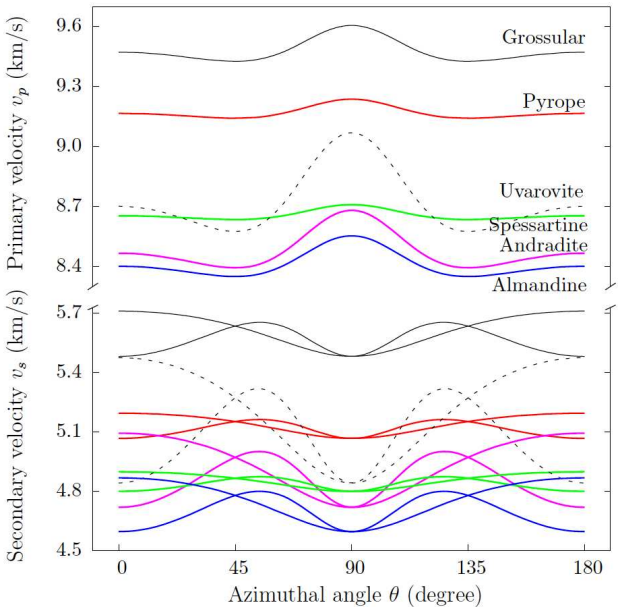

Fig. 2 (color online) Directional seismic wave velocities of the six silicate garnet end-members here considered, as computed *ab initio* in the present study. Quasi-longitudinal v_p and quasi-transverse v_s velocities are reported (in the upper and lower part of the plot, respectively) along the azimuthal angle θ defined in the inset of Figure 1.

Pyr < Gro. Grossular and pyrope allow for the fastest propagation of primary elastic waves while almandine and andradite for the slowest one. This behavior can be deduced directly from the analysis of the elemental composition of the end-members and from relations (5); indeed, seismic wave velocities are inversely proportional to the density ρ of the material. Fe-bearing phases, such as almandine and andradite, are the most dense, followed by Mn- and Cr-bearing phases, such as spessartine and uvarovite; grossular and pyrope contains the lightest elements (Mg, Al and Ca) among the six end-members and are then less dense.

3.2 From End-members to Solid Solutions

It was recalled in the Introduction that natural silicate garnets form solid solutions in a wide range of chemical compositions. In this subsection, we analyze how linearly *ab initio* computed bulk moduli of the pure end-members can be used to compute bulk moduli of solid solutions of any compositions. It has already been inferred that quasi-linear composition-bulk modulus trends are expected for garnets in the pyralspite system (Isaak and Graham, 1976; Duffy and Anderson, 1989; Yeganeh-Haeri et al, 1990) where the bulk moduli of the corresponding end-members are relatively close to one another; whereas large deviations from linearity have been suggested for solid solutions between grossular and andradite (Babuška et al, 1978; O'Neill et al, 1989). Solid solutions between pyralspites and ugrandites are rare in natural garnets (Hensen, 1976).

In order to compare with experiment, we consider the set of 32 solid solutions of the pyralspite system and 4 solid solutions of the ugrandite system reported by Wang and Ji (2001). In Table 3, we report the experimental bulk moduli of these solid solutions and the corresponding theoretical values, computed from the *ab initio* bulk moduli for the pure end-members (data reported in Table 2) by assuming a linear relation between chemical composition and elastic properties. For each solid solution, the percentage deviation Δ from the experimental data is also reported.

For the pyralspite solid solutions, the agreement between experimental and theoretical values is rather good, with an overall percentage deviation of 1.0 %, that is comparable with the uncertainty related to the description of the elastic properties of pure end-members. Furthermore, most of the largest deviations ($\geq$ 1.9 %) refer to relatively old experimental data. It is then confirmed that, by performing accurate ab initio calculations of the elastic properties of the end-members, the bulk modulus of pyralspite solid solutions of any composition can be predicted accurately as well. The situation is completely different as regards ugrandite solid solutions. In this case, even if the dataset in Table 3 is small, a clear deviation from the linear behavior is observed, with an overall disagreement of 5.1 %. In order to correctly predict the elastic properties of grossular-andradite solid solutions, rather complex calculations are required that explicitly consider the various chemical compositions. These calculations are currently being performed and their results will be presented in a forthcoming paper.

4 Final Remarks

Accurate *ab initio* simulations of the elastic properties of six silicate garnet end-members have been performed. A full characterization of their elastic tensors, seismic wave velocity anisotropy and polycrystalline average elastic properties is reported. The linear transferability of the bulk modulus from end-members to solid solutions of different chemical compositions is confirmed for pyralspites while large deviations from linearity are observed for ugrandites.

The results presented in this study clearly demonstrate that a reliable description of the elastic properties of garnets, at ambient pressure, can be obtained from accurate *ab initio* simulations, including a detailed

description of the elastic wave anisotropy. We are currently devising a computational scheme for the inclusion of the effect of pressure on computed elastic properties of crystals and applying it to the case of silicate garnets, in order to study them at pressures of geophysical interest.

Acknowledgements The authors want to express their gratitude to Dr. Donato Belmonte for kind and enlightening discussions. Ms. Elisa Albanese is kindly acknowledged for her contribution to the implementation of the Christoffel's equation. The CINECA Award N. HP10BLSOR4-2012 is acknowledged for the availability of high performance computing resources and support. Improvements of the CRYSTAL09 code in its massive-parallel version was made possible thanks to the PRACE proposal no. 2011050810.

References

Anderson DL (1989) Theory of the Earth. Blackwell Scientific Publications, Boston

Anderson DL, Bass JD (1986) Transition region of the earth's upper mantle. Nature 320:321–328

Auld BA (1973) Acoustic Fields and Waves in Solids. Krieger Publishing Company, Malabar, Florida

Authier A, Zarembowitch A (2006) Elastic properties. In: Authier A (ed) International Tables for Crystallography, Vol. D, Wiley, p 72

Babuška V, Fiala J, Kumazawa M, Ohno I, Sumino Y (1978) Elastic properties of garnet solid-solution series. Phys Earth Planet Int 16:157–176

Baima J, Erba A, Orlando R, Rérat M, Dovesi R (2013) Beryllium oxide nanotubes and their connection to the flat monolayer. J Phys Chem C 117:12864–12872

Bass JD (1986) Elasticity of uvarovite and andradite garnets. J Geophys Res 91:7505–7516

Bass JD (1989) Elasticity of grossular and spessartite garnets by brillouin spectroscopy. J Geophys Res 94:7621–7628

Bass JD, Anderson DL (1984) Composition of the upper mantle: Geophysical tests of two petrological models. Geophys Res Lett 11:229–232

Becke AD (1993) Density-functional thermochemistry III. The role of exact exchange. J Chem Phys 98:5648

Belmonte D, Ottonello G, Zuccolini MV (2013) Melting of α-Al_2O_3 and vitrification of the undercooled alumina liquid: Ab initio vibrational calculations and their thermodynamic implications. J Chem Phys 138(6):064507

Bonczar LJ, Graham EK, Wang H (1977) The pressure and temperature dependence of the elastic constants of pyrope garnet. J Geophys Res 82:2529–2534

Broyden CG (1970) The convergence of a class of double-rank minimization algorithms 1. General considerations. J Inst Math Appl 6:76–90

Chai M, Brown JM, Slutsky LJ (1997) The elastic constants of a pyrope-grossular-almandine garnet to 20 GPa. Geophys Res Lett 24:523–526

Chen G, Miletich R, Mueller C, Spetzler HA (1997) Shear and compressional mode measurements with GHz ultrasonic interferometry and velocity-composition systematics for the pyrope-almandine solid solution series. Phys Earth Planet Int 99:273–287

Chen G, Cooke JA, Gwanmesia GD, Liebermann RC (1999) Elastic wave velocities of $Mg_3Al_2Si_3O_{13}$-pyrope garnet to 10 GPa. Am Miner 84:384–388

Chopelas A, Reichmann HJ, Zhang L (1996) Sound velocities of five minerals to mantle pressures determined by the sideband fluorescence method. In: Dyar MD, McCammon C, Schaefer MW (eds) Mineral Spectroscopy, Geochem. Soc., Washington, D.C., p 229

Civalleri B, D'Arco P, Orlando R, V R Saunders RD (2001) Hartree-Fock geometry optimisation of periodic systems with the crystal code. Chem Phys Lett 348:131–138

Dal Corso A, Posternak M, Resta R, Baldereschi A (1994) Ab initio study of piezoelectricity and spontaneous polarization in ZnO. Phys Rev B 50:10715–10721

D'Arco P, Freyria Fava F, R Dovesi VRS (1996) Structural and electronic properties of pyrope garnet: An ab initio study. J Phys: Condens Matter 8:8815

Doll K (2001) Implementation of analytical Hartree-Fock gradients for periodic systems. Comput Phys Commun 137:74–88

Doll K, Saunders V, Harrison N (2001) Analytical Hartree-Fock gradients for periodic systems. Int J Quantum Chem 82:1–13

Dovesi R, Orlando R, Civalleri B, Roetti C, Saunders VR, Zicovich-Wilson CM (2005) Crystal: a computational tool for the ab initio study of the electronic properties of crystals. Z Kristallogr 220:571–573

Dovesi R, Saunders VR, Roetti C, Orlando R, Zicovich-Wilson CM, Pascale F, Doll K, Harrison NM, Civalleri B, Bush IJ, D'Arco P, Llunell M (2010) `CRYSTAL09` User's Manual. Università di Torino, Torino, http://www.crystal.unito.it

Dovesi R, De La Pierre M, Ferrari AM, Pascale F, Maschio L, Zicovich-Wilson CM (2011) The IR vibrational properties of six members of the garnet family: A quantum mechanical ab initio study. Am Mineral 96:1787–1798

Duffy TS, Anderson DL (1989) Seismic velocities in mantle minerals and the mineralogy of the upper mantle. J Geophys Res 94:1895–1912

Erba A, Dovesi R (2013) Photoelasticity of crystals from theoretical simulations. Phys Rev B 88:045121

Erba A, El-Kelany KE, Ferrero M, Baraille I, Rérat M (2013a) Piezoelectricity of $SrTiO_3$: An ab initio description. Phys Rev B 88:035102

Erba A, Ferrabone M, Baima J, Orlando R, Rérat M, Dovesi R (2013b) The vibration properties of the (n,0) boron nitride nanotubes from ab initio quantum chemical simulations. J Chem Phys 138:054906

Fletcher R (1970) A new approach to variable metric algorithms. Comput J 13:317–322

Goldfarb D (1970) A family of variable-metric methods derived by variational means. Math Comput 24:23–26

Goto T, Ohno I, Sumino Y (1976) The determination of elastic constants of natural pyrope-almandine garnet by means of rectangular parallelepiped resonance method. Phys Earth 24:149–158

Halleck PM (1973) The compression and compressibility of grossular garnet: A comparison of x-ray and ultrasonic methods. PhD dissertation p 82

Hensen BJ (1976) The stability of pyrope-grossular garnet with excess silica. Contrib Mineral Petrol 55:279–292

Hill R (1963) Elastic properties of reinforced solids: Some theoretical principles. J Mech Phys Solids 11:357–372

Isaak DG, Graham EK (1976) The elastic properties of an almandine-spessartine garnet and elasticity in the garnet solid solution series. J Geophys Res 81:2483–2489

Jiang F, Speziale S, Shieh SR, Duffy TS (2004) Single-crystal elasticity of andradite garnet to 11 GPa. J Phys:Condens Matter 16:S1041

Karki BB, Stixrude L, Clark SJ, Warren MC, Ackland GJ, Crain J (1997) Structure and elasticity of MgO at high pressure. Am Mineral 82:51–60

Karki BB, Stixrude L, Wentzcovitch RM (2001) High-pressure elastic properties of major materials of earth's mantle from first principles. Rev Geophys 39:507–534

Kawai K, Tsuchiya T (2012) First principles investigations on the elasticity and phase stability of grossular garnet. J Geophys Res: Solid Earth 117:B02,202

Koch W, Holthausen MC (2000) A Chemist's Guide to Density Functional Theory. Wiley-VCH Verlag, Weinheim (Federal Republic of Germany)

Lacivita V, D'Arco P, Orlando R, Dovesi R, Meyer A (2013a) Anomalous birefringence in andradite-grossular solid solutions. A quantum-mechanical approach. Phys Chem Minerals, in press

Lacivita V, Erba A, Noël Y, Orlando R, D'Arco P, Dovesi R (2013b) Zinc oxide nanotubes: An ab initio investigation of their structural, vibrational, elastic, and dielectric properties. J Chem Phys 138:214706

Lee C, Yang W, Parr RG (1988) Development of the Colle-Salvetti correlation-energy formula into a functional of the electron density. Phys Rev B 37:785–789

Leitner BJ, Weidner DJ, Liebermann RC (1980) Elasticity of single crystal pyrope and implications for garnet solid solution series. Phys Earth Planet Int 22:111–121

Li L, Weidner DJ (2011) Ab initio molecular dynamic simulation of the elasticity of $Mg_3Al_2Si_3O_{12}$ pyrope. J Earth Science 22:169–175

Lu C, Mao Z, Lin JF, Zhuravlev KK, Tkachev SN, Prakapenka VB (2013) Elasticity of single-crystal iron-bearing pyrope up to 20 GPa and 750 K. Earth and Planetary Science Letters 361(0):134 – 142

Meyer A, Pascale F, Zicovich-Wilson CM, Dovesi R (2010) Magnetic interactions and electronic structure of uvarovite and andradite garnets. an ab initio all-electron simulation with the `CRYSTAL06` program. Int J Quantum Chem 110(2):338–351

Mittal R, Chaplot SL, Choudhury N (2001) Lattice dynamics calculations of the phonon spectra and thermodynamic properties of the aluminosilicate garnets pyrope, grossular, and spessartine $M_3Al_2Si_3O_{12}$ (M=Mg, Ca, and Mn). Phys Rev B 64:094302

Musgrave MJP (1970) Crystal Acoustics. Holden-Day, San Francisco, California

Novak GA, Gibbs GV (1971) The crystal chemistry of the silicate garnets. Am Mineral 56:791–825

Nye JF (1957) Physical properties of crystals. Oxford University Press, Oxford

O'Neill B, Bass JD, Smyth JR, Vaughan MT (1989) Elasticity of a grossular-pyrope-almandine garnet. J Geophys Res 94:17819–17824

O'Neill B, Bass JD, Rossman GR, Geiger CA, Langer K (1991) Elastic properties of pyrope. Phys Chem Miner 17:617–621

Ottonello G, Civalleri B, Ganguly J, Perger WF, Belmonte D, Vetuschi Zuccolini M (2010) Thermochemical and thermo-physical properties of the high-pressure phase anhydrous b ($Mg_{14}Si_5O_{24}$): An ab-initio all-electron investigation. Am Mineral 95:563–573

Pascale F, Zicovich-Wilson C, Orlando R, Roetti C, Ugliengo P, Dovesi R (2005) Vibration frequencies of $Mg_3Al_2Si_3O_{12}$ pyrope. an ab initio study with the crystal code. J Phys Chem B 109:6146–6152

Pavese A (1999) Quasi-harmonic computer simulations of the structural behaviour and EOS of pyrope at

high pressure and high temperature. Phys Chem Miner 26:649–657

Perger WF, Criswell J, Civalleri B, Dovesi R (2009) Ab-initio calculation of elastic constants of crystalline systems with the crystal code. Comput Phys Commun 180:1753–1759

Rickwood PC, Mathias M, Siebert JC (1968) A study of garnets from eclogite and peridotite xenoliths found in kimberlite. Contrib Mineral Petrol 19:271–301

Ringwood AE (1975) Composition and Petrology of the Earth's Mantle. McGraw-Hill, New York

Saghi-Szabo G, Cohen RE, Krakauer H (1998) First-principles study of piezoelectricity in $PbTiO_3$. Phys Rev Lett 80:4321–4324

Shanno DF (1970) Conditioning of quasi-newton methods for function minimization. Math Comput 24:647–656

Sinogeikin SV, Bass JD (2000) Single-crystal elasticity of pyrope and MgO to 20 GPa by Brillouin scattering in the diamond cell. Phys Earth Planet Int 120:43–62

Soga N (1967) Elastic constants of garnet under pressure and temperature. J Geophys Res 72:4227–4234

Sumino Y, Anderson LO (1982) Elastic constants of minerals. In: Carmichael RS (ed) Handbook of Physical Properties of Rocks, CRC Press, Boca Raton, Florida, p 39

Suzuki I, Anderson OL (1983) Elasticity and thermal expansion of a natural garnet up to 1000 K. J Phys Earth 31:125–138

Tosoni S, Pascale F, Ugliengo P, Orlando R, Saunders VR, Dovesi R (2005) Quantum mechanical calculation of the oh vibrational frequency in crystalline solids. Mol Phys 103:2549–2558

Tsuchiya T, Kawamura K (2001) Systematics of elasticity: Ab initio study in b1-type alkaline earth oxides. J Chem Phys 114:10086

Valenzano L, Meyer A, Demichelis R, Civalleri B, Dovesi R (2009) Quantum-mechanical ab initio simulation of the Raman and IR spectra of $Mn_3Al_2Si_3O_{12}$ spessartine. Phys Chem Minerals 36(7):415–420

Valenzano L, Pascale F, Ferrero M, Dovesi R (2010) Ab initio quantum-mechanical prediction of the IR and Raman spectra of $Ca_3Cr_2Si_3O_{12}$ uvarovite garnet. Int J Quantum Chem 110(2):416–421

Verma RK (1960) Elasticity of some high-density crystals. J Geophys Res 65:757–766

Wang H, Simmons G (1974) Elasticity of some mantle crystal structures 3. spessartite-almandine garnet. J Geophys Res 79:2607–2613

Wang Z, Ji S (2001) Elasticity of six polycrystalline silicate garnets at pressure up to 3.0 GPa. Am Miner 86:1209–1218

Webb SL (1989) The elasticity of the upper mantle orthosilicates olivine and garnet to 3 GPa. Phys Chem Minerals 16:684–692

Winkler B, Dove MT, Leslie M (1991) Static lattice energy minimization and lattice dynamics calculations on aluminosilicate minerals. Am Mineral 76:313–331

Yeganeh-Haeri A, Weidner DJ, Ito E (1990) Elastic properties of the pyrope-majorite solid solution series. Geophys Res Lett 17:2453–2456

Zicovich-Wilson CM, Torres FJ, Pascale F, Valenzano L, Orlando R, Dovesi R (2008) Ab initio simulation of the IR spectra of pyrope, grossular, and andradite. J Comput Chem 29:2268–2278

Table 3 Comparison between experimental bulk modulus of a set of solid solutions of different chemical composition among the six silicate garnet end-members here considered and *ab initio* computed ones from the bulk moduli of pure end-members, assuming a linear relation between composition and bulk modulus. For each solid solution, the percentage deviation Δ from the experimental data is reported. The averaged absolute-value percentage deviation $|\overline{\Delta}|$ is also reported for solid solutions of the pyralspite and ugrandite families.

	Ref.	K_{exp} (GPa)	K_{calc} (GPa)	Δ (%)
$Alm_{43}Spe_{55}Gro_2$	Verma (1960)	174.9	176.8	1.1
$Alm_{46}Spe_{54}$	Wang and Simmons (1974)	177.2	176.8	-0.2
$Alm_{46}Spe_{54}$	Isaak and Graham (1976)	177.7	176.8	-0.5
$Pyr_{14}Alm_{81}Gro_5$	Verma (1960)	176.7	173.4	-1.9
$Pyr_{14}Alm_{81}Spe_5$	Sumino and Anderson (1982)	176.4	173.8	-1.5
$Pyr_1Alm_{44}Spe_{55}$	Sumino and Anderson (1982)	175.5	176.8	0.7
$Pyr_{20}Alm_{74}Spe_3Gro_3$	Soga (1967)	177.0	173.4	-2.0
$Pyr_{20}Alm_{74}Spe_6$	Sumino and Anderson (1982)	177.0	173.7	-1.9
$Pyr_{22}Alm_{64}Spe_{11}And_2$	Babuška et al (1978)	176.8	173.4	-1.9
$Pyr_{22}Alm_{64}Spe_{14}$	Sumino and Anderson (1982)	176.8	174.0	-1.6
$Pyr_{22}Alm_{72}Spe_6$	Chen et al (1997)	173.6	173.0	0.4
$Pyr_{25}Alm_{56}Spe_{19}$	Wang and Ji (2001)	172.4	174.2	1.0
$Pyr_{28}Alm_{60}Spe_{12}$	Sumino and Anderson (1982)	175.4	173.7	-1.0
$Pyr_2Alm_{46}Spe_{52}$	Sumino and Anderson (1982)	176.3	176.6	0.2
$Pyr_{35}Alm_{50}Spe_7Gro_8$	Sumino and Anderson (1982)	174.7	173.0	-1.0
$Pyr_{39}Alm_{51}Spe_9Gro_1$	Sumino and Anderson (1982)	173.4	173.2	-0.1
$Pyr_{39}Alm_{54}Spe_4Gro_3$	Sumino and Anderson (1982)	173.6	172.9	-0.4
$Pyr_{41}Alm_{48}Spe_7Gro_4$	Sumino and Anderson (1982)	174.9	173.0	-1.1
$Pyr_{50}Alm_{46}Gro_4$	Sumino and Anderson (1982)	173.3	172.3	-0.6
$Pyr_{52}Alm_{32}Gro_{16}$	Chai et al (1997)	174.1	171.9	-1.3
$Pyr_{55}Alm_{37}Spe_2Gro_6$	Goto et al (1976)	172.2	172.2	0.0
$Pyr_{57}Alm_{28}Gro_{15}$	Chen et al (1997)	175.0	171.8	-1.8
$Pyr_{60}Alm_{31}Gro_9$	Bonczar et al (1977)	177.0	171.9	-2.9
$Pyr_{61}Alm_{36}Gro_2$	Sumino and Anderson (1982)	175.5	172.1	-2.0
$Pyr_{61}Alm_{36}Spe_3$	Webb (1989)	168.2	170.3	1.3
$Pyr_{62}Alm_{36}Gro_2$	Sumino and Anderson (1982)	173.6	172.0	-0.9
$Pyr_{70}Alm_{16}Spe_9Gro_5$	Sumino and Anderson (1982)	170.8	172.2	0.8
$Pyr_{73}Alm_{14}Spe_5Gro_8$	Suzuki and Anderson (1983)	171.6	171.8	0.1
$Pyr_{73}Alm_{16}And_4Uva_6$	Sumino and Anderson (1982)	171.2	169.9	-0.8
$Pyr_{73}Alm_{16}Spe_6Gro_5$	Sumino and Anderson (1982)	171.3	172.0	0.4
$Pyr_7Alm_{18}Spe_{75}$	Sumino and Anderson (1982)	176.4	177.7	0.7
$Pyr_{90}Alm_8Gro_2$	O'Neill et al (1991)	173.0	173.9	0.5
$Pyr_{97}Alm_2$	Chen et al (1997)	170.3	171.0	0.4
$\|\overline{\Delta}\|$ (%)		-	-	1.0
$Gro_{22}And_{70}$	Sumino and Anderson (1982)	147.3	156.6	6.3
$Gro_{22}And_{70}Pyr_3Alm_4$	Babuška et al (1978)	147.3	157.7	7.1
$Gro_{76}And_{22}$	Sumino and Anderson (1982)	162.4	166.7	2.6
$Gro_{80}And_{14}$	Sumino and Anderson (1982)	161.2	168.1	4.3
$\|\overline{\Delta}\|$ (%)		-	-	5.1